BAYESIAN JOINT DETECTION-ESTIMATION OF BRAIN ACTIVITY USING MCMC WITH A GAMMA-GAUSSIAN MIXTURE PRIOR MODEL

Salima Makni,[1] *Philippe Ciuciu,*[1] *Jérôme Idier,*[2] *and Jean-Baptiste Poline*[1]

[1]Service Hospitalier Frédéric Joliot (CEA) 4, Place du Général Leclerc, 91406 Orsay, France
[2]IRCCyN (CNRS), 1 rue de la Noë, BP 92101 44321 Nantes cedex 3, France
[1] name@shfj.cea.fr, [2] Jerome.Idier@irccyn.ec-nantes.fr

ABSTRACT

The classical approach of within-subject analysis in event-related functional Magnetic Resonance Imaging (fMRI) first relies on (i) a detection step to localize which parts of the brain are activated by a given stimulus type, and then on (ii) an estimation step to recover the temporal dynamics of the brain response. To date, specially in region-based analysis, the two questions have been addressed separately while intrinsically connected to each other. This situation motivates the need for new methods in neuroimaging that go beyond this unsatisfactory trade-off. In this paper, we propose a generalization of a region based Bayesian detection-estimation approach that addresses (i)-(ii) simultaneously as a bilinear inverse problem. The proposed extension relies on a 2-class Gamma-Gaussian prior mixture modeling to classify the voxels of the brain region either as activated or unactivated. Our approach provides both a spatial activity map and a HRF estimation using Monte Carlo Markov Chain (MCMC) techniques. Results show that this novel mixture model yields lower false positive rates and a better sensitivity in comparison with a 2-class Gaussian mixture.

1. INTRODUCTION

Many studies in fMRI aim to localize brain regions for which the signal fluctuations correlate with the stimulus or subject task. In event-related fMRI, complementary analysis allows us to recover the temporal dynamics of the brain response [1, 2]. Up to now, these questions have been addressed sequentially. In [3], a novel detection estimation approach was proposed to perform these two tasks simultaneously in a region-based analysis. Within the Bayesian framework, we first integrated physiological prior information to obtain a slow-varying time course as an estimate of the shape of the Hemodynamic Response Function (HRF). We also considered a mixture of two Gaussian probability density function (pdf) as a prior model on the "neural" response levels (NRL) to accomodate the voxel and task-dependent variations within the ROI. Reliable results have been obtained on real fMRI data in regions of interest (ROI) where most voxels were actually activated for a given stimulus type. We also noted that when the chosen ROI was not involved by a given stimulus type, high false positive rates were observed. A thorough analysis showed that the conditional posterior pdf of the NRLs, which is also a two-class Gaussian mixture, consisted of distributions too close to be distinguishable. In this paper, we propose an extension of this method to cope with this issue : our goal is to obtain a more robust classification of the two classes and an improved estimation of all parameters. To this end, we introduce a Gamma-Gaussian mixture prior model on the NRLs and derive the target posterior pdf as well as posterior mean estimates (PMEs) of all the parameters of interest and hyperparameters. These estimates are directly computed from the generated samples using a Gibbs sampler algorithm. This approach is tested both on synthetic and real fMRI data. Compared to [3], a significant gain is achieved in terms of specificity (lower false positive rate) and sensitivity (lower false negative rate).

2. MODEL

2.1. Formulation

Let us define $\boldsymbol{y}_j = (y_{j,t_n})_{n=1:N}$ as the fMRI time course measured in voxel V_j at time t_n. Here, a functionally homogeneous ROI $\mathcal{R} = (V_j)_{j=1:J}$ is first characterized by a single HRF shape $\boldsymbol{h} = (h_{d\tau})_{d=0:D}$ ($D+1$ is the number of HRF coefficients and τ is the sampling interval of the trial onsets) and second by task and voxel dependent magnitude adjustment described by parameter a_j^m for voxel V_j and condition m. Then the model reads :

$$\boldsymbol{y}_j = \sum_{m=1}^{M} a_j^m \boldsymbol{X}^m \boldsymbol{h} + \boldsymbol{P}\ell_j + \boldsymbol{b}_j, \quad \forall\, j = 1:J, \qquad (1)$$

where $\boldsymbol{X}^m = (x^m_{t_n - d\tau})_{n=1:N}^{d=0:D}$ is a binary matrix corresponding to the arrival times for the mth condition. Note that $\boldsymbol{P}\ell_j$ models the trend and $\boldsymbol{b}_j \sim \mathcal{N}(0, \epsilon_j^2)$ stands for the noise. Here for simplicity, we have just considered a *spatially varying* Gaussian white noise model. A more sophisticated model could be introduced using autoregressive processes to account for the serial correlation of the fMRI time series as done in [4].

2.2. Likelihood

We assume that the fMRI time series $\boldsymbol{y} = (\boldsymbol{y}_j)_{j=1:J}$ are iid in space, so the likelihood function reads :

$$p(\boldsymbol{y} \,|\, \boldsymbol{h}, \boldsymbol{a}, \boldsymbol{\ell}, \boldsymbol{\epsilon}^2) \propto \prod_{j=1}^{J} \epsilon_j^{-N} \exp\Big(-\frac{1}{2\epsilon_j^2} \big\| \widetilde{\boldsymbol{y}}_j - \boldsymbol{P}\ell_j \big\|^2\Big),$$

where $\widetilde{\boldsymbol{y}}_j = \boldsymbol{y}_j - \sum_m a_j^m \boldsymbol{X}^m \boldsymbol{h}$.

3. THE DETECTION-ESTIMATION PROBLEM

Assuming that the given ROI has homogeneous vasculature properties, we propose to estimate a single HRF shape $\boldsymbol{h}$ and the corresponding NRLs. Our aim is also to classify voxels of the ROI

either as activated or not. Following [5, 6], a two-class mixture model on the NRLs has been introduced in [3]. For every condition m, 2 Gaussian priors have been considered : one for activated voxels (class 1) and the other for unactivated ones (class 0). With respect to the NRLs, the posterior distribution is also a Gaussian mixture. When the main part of the ROI is not activated, we observed that this posterior mixture is almost degenerated in the sense that some voxels are randomly assigned to class 1 while they may correspond to unactivated areas. Here, we propose to solve this problem by choosing a more appropriate prior model for the NRLs. We choose two different pdfs for the conditional distributions of the NRL given the class. We keep a Gaussian pdf for unactivated voxels, while we consider a Gamma pdf for activated ones. Doing so, negative NRLs are forbidden in class 1, meaning that activations are modelled by non-negative NRLs. In what follows, we give all the available prior information, we derive the joint posterior distribution and summarize the estimation approach.

3.1. Prior information

The HRF. According to [7, 8], the HRF can be characterized as a causal slow-varying function which returns to its baseline after about 25 sec. These assumptions lead us to select a Gaussian prior on $\boldsymbol{h} \sim \mathcal{N}(\boldsymbol{0}, \|\partial^2 \boldsymbol{h}\|^2/2\sigma_{\boldsymbol{h}}^2)$, where :

$$(\partial^2 \boldsymbol{h})_{d\tau} \approx (h_{(d+1)\tau} - 2h_{d\tau} + h_{(d-1)\tau})/\tau^2, \forall d = 1 : D-1.$$

The "neural" response levels. We assume that different types of conditions induce statistically independent NRLs *i.e.,* $p(\boldsymbol{a}; \boldsymbol{\theta_a}) = \prod p(\boldsymbol{a}^m; \boldsymbol{\theta}_m)$ with $\boldsymbol{a} = (\boldsymbol{a}^m)_{m=1:M}$, $\boldsymbol{a}^m = (a_j^m)_{j=1:J}$ and $\boldsymbol{\theta_a} = (\boldsymbol{\theta}_m)_{m=1:M}$. Vector $\boldsymbol{\theta}_m$ denotes the set of unknown hyperparameters related to the mth stimulus type.
Since only a few voxels of the ROI may be activated by a given condition, we introduce couples of random variables $z_j^m = (q_j^m, a_j^m)_{j=1:J}^{m=1:M}$ where q_j^m is a binary random variable that indicates whether voxel V_j is activated ($q_j^m = 1$) or not ($q_j^m = 0$) by condition m.
Conditional on $q_j^m = 0$, a_j^m is modelled as a Gaussian random variable : $p(a_j^m \,|\, q_j^m = 0) \sim \mathcal{N}(0, v_{0,m})$. In contrast, when $q_j^m = 1$, a_j^m is modelled as a Gamma random variable to encode non-negativity of the response for voxel V_j and condition m ($p(a_j^m \,|\, q_j^m = 1) \sim \mathcal{G}(\alpha_m, \beta_m)$). We thus introduce a Gamma-Gaussian prior mixture :

$$p(a_j^m \,|\, \boldsymbol{\theta}_m) = \sum_{i=0,1} \Pr(q_j^m = i \,|\, \lambda_m)\, p(a_j^m \,|\, q_j^m = i, \boldsymbol{\theta}_m),$$

with $\Pr(q_j^m = 1) = \lambda_m$, $\Pr(q_j^m = 0) = \bar{\lambda}_m = 1 - \lambda_m$ and $\boldsymbol{\theta}_m = [\lambda_m, \alpha_m, \beta_m, v_{0,m}]$. $\mu_{0,m} = 0$ since it represents the mean of the NRLs for unactivated voxels.

The low-frequency drift. Vector $\boldsymbol{\ell} = (\ell_j)_{j=1:J}$ defines the unknown parameters of the orthonormal basis function $\boldsymbol{P}$. We assume that $\boldsymbol{\ell}$ is a random process independent of $\boldsymbol{h}$ such that $p(\boldsymbol{\ell}; \sigma_\ell^2) = \prod_j p(\ell_j; \sigma_\ell^2)$ and $\ell_j \sim \mathcal{N}(\boldsymbol{0}, \sigma_\ell^2 \boldsymbol{I}_Q)$. In this paper, calculations are derived in the non informative case, that is when $\sigma_\ell^2 \to +\infty$.

The hyperparameters. The complete set of hyperparameters to be estimated is denoted $\boldsymbol{\Theta} = \big[\boldsymbol{\epsilon}^2, \sigma_{\boldsymbol{h}}^2, \boldsymbol{\theta_a}\big]$. Without informative prior knowledge, we consider the following priors for these parameters : $p(\epsilon_j^2, \sigma_{\boldsymbol{h}}^2) = (\epsilon_j \sigma_{\boldsymbol{h}})^{-1}$, $p(\boldsymbol{\theta}_m) \propto a \exp(-a\, \alpha_m)\, \mathcal{G}(\beta_m, b, c)\ (v_{0,m} \lambda_m \bar{\lambda}_m)^{-1/2}$. Values of a, b and c are fixed empirically.

3.2. The joint posterior distribution

Considering the constructed model and assuming no further prior dependence between parameters, formal application of the chain rule yields :

$$p(\boldsymbol{h}, \boldsymbol{a}, \boldsymbol{\ell}, \boldsymbol{\Theta} \,|\, \boldsymbol{y}) \propto p(\boldsymbol{y} \,|\, \boldsymbol{h}, \boldsymbol{a}, \boldsymbol{\ell}, \boldsymbol{\epsilon}^2)\, p(\boldsymbol{a} \,|\, \boldsymbol{\theta_a})\, p(\boldsymbol{h} \,|\, \sigma_{\boldsymbol{h}}^2)\, p(\boldsymbol{\ell})\, p(\boldsymbol{\Theta}).$$

Here, we choose to integrate analytically the nuisance variables $\boldsymbol{\ell}$:

$$p(\boldsymbol{h}, \boldsymbol{a}, \boldsymbol{\Theta} \,|\, \boldsymbol{y}) \propto \Big(\prod_j \epsilon_j^{-N-1+Q}\Big) \sigma_{\boldsymbol{h}}^{-D} \exp\Big(-\frac{\boldsymbol{h}^{\mathrm{t}} \boldsymbol{R}^{-1} \boldsymbol{h}}{2\sigma_{\boldsymbol{h}}^2}\Big) \exp\Big(-\frac{\sum_j \widetilde{\boldsymbol{y}}_j^{\mathrm{t}} \boldsymbol{Q}_j \widetilde{\boldsymbol{y}}_j}{2}\Big) \prod_m \Big(p(\boldsymbol{\theta}_m) \prod_j p(a_j^m \,|\, q_j^m, \boldsymbol{\theta}_m)\Big). \quad (2)$$

with $\boldsymbol{Q}_j = \big(\boldsymbol{I}_N - \boldsymbol{P}\boldsymbol{P}^{\mathrm{t}}\big)/\epsilon_j^2$.
To get samples from this posterior pdf, we use a Gibbs sampler which consists in building a Markov chain, whose target distribution is (2), by sequentially generating random samples from the full conditional pdfs of all the unknown parameters and hyperparameters. Finally, PMEs are computed from these realizations after considering a burn-in period. The sampling scheme for the different variables $(\boldsymbol{h}, \boldsymbol{a}, \boldsymbol{\Theta})$ is detailed in the next paragraph.

3.3. Computational details

3.3.1. The HRF and its scale.

Let us denote $\boldsymbol{S}_j = \sum_m a_j^m \boldsymbol{X}^m$. $\boldsymbol{h}$ is $\mathcal{N}(\boldsymbol{\mu_h}, \boldsymbol{\Sigma_h})$-distributed with : $\boldsymbol{\Sigma_h}^{-1} = \sigma_{\boldsymbol{h}}^{-2} \boldsymbol{R}^{-1} + \sum_j \boldsymbol{S}_j^{\mathrm{t}} \boldsymbol{Q}_j \boldsymbol{S}_j$ and $\boldsymbol{\mu_h} = \boldsymbol{\Sigma_h} \sum_j \boldsymbol{S}_j^{\mathrm{t}} \boldsymbol{Q}_j \boldsymbol{y}_j$.
Sampling the scale $\boldsymbol{\sigma}_{\boldsymbol{h}}^2$ amounts to simulating according to $p(\boldsymbol{\sigma}_{\boldsymbol{h}}^2 \,|\, \boldsymbol{h}) \sim \mathcal{IG}\big(D/2, \boldsymbol{h}^{\mathrm{t}} \boldsymbol{R}^{-1} \boldsymbol{h}/2\big)$.

3.3.2. The "neural" response levels.

Sampling the mixture is done sequentially for each voxel V_j and condition m and using two nested loops, the inner corresponding to the stimulus types (*e.g.,* index m) and the outer to voxels (*e.g.,* index j). We first start with sampling the class (parameter q_j^m) and then sampling the NRL a_j^m conditionally to q_j^m. These two steps are as follows. First, the posterior mixture reads :

$$p(a_j^m \,|\, rest) \propto p(\lambda_m) \exp\Big(-\frac{1}{2} \big\|\boldsymbol{e}_{j,m} - a_j^m \boldsymbol{g}_m\big\|_{\boldsymbol{Q}_j}^2\Big) \times \Big(\lambda_m\, p(a_j^m \,|\, q_j^m = 1, \alpha_m, \beta_m)\, p(\alpha_m, \beta_m) + \bar{\lambda}_m\, p(a_j^m \,|\, q_j^m = 0, v_{0,m})\, p(v_{0,m})\Big), \quad (3)$$

with : *rest* = remaining variables, $\boldsymbol{g}_m = \boldsymbol{X}^m \boldsymbol{h}$, and $\boldsymbol{e}_{j,m} = \boldsymbol{y}_j - \sum_{n \neq m} a_j^n \boldsymbol{g}_n$. After some calculations, (3) becomes :

$$p(a_j^m \,|\, rest) \propto \frac{\lambda_{0,j}^m}{(2\pi v_{0,j}^m)^{1/2}} \exp\Big(-\frac{\big(a_j^m - \mu_{0,j}^m\big)^2}{2v_{0,j}^m}\Big) + \frac{\lambda_{1,j}^m}{K} (a_j^m)^{\alpha_m - 1} \exp\Big(-\frac{\big(a_j^m - \mu_{1,j}^m\big)^2}{2v_{1,j}^m}\Big) \mathbb{I}_{\mathbb{R}^+}(a_j^m) \quad (4)$$

with

$$\lambda_{i,j}^m = \left(1 + \tilde{\lambda}_{1-i,j}^m / \tilde{\lambda}_{i,j}^m\right)^{-1}, \quad i = 0, 1$$

$$\tilde{\lambda}_{0,j}^m = \frac{\bar{\lambda}_m^{1/2} (v_{0,j}^m)^{1/2}}{\lambda_m^{1/2}\, v_{0,m}} \exp\left(\frac{(\mu_{0,j}^m)^2}{2 v_{0,j}^m}\right),$$

$$\tilde{\lambda}_{1,j}^m = p(\alpha_m)\, p(\beta_m) \frac{\beta_m^{\alpha_m} \lambda_m^{1/2} K}{\Gamma(\alpha_m) \bar{\lambda}_m^{1/2}} \exp\left(\frac{(\mu_{1,j}^m)^2}{2 v_{1,j}^m}\right),$$

$$K = \int_0^{+\infty} (a_j^m)^{\alpha_m - 1} \exp\left(-\frac{\left(a_j^m - \mu_{1,j}^m\right)^2}{2 v_{1,j}^m}\right) d\, a_j^m.$$

with : $v_{0,j}^m = \left(v_{0,m}^{-1} + \boldsymbol{g}_m^{\mathrm{t}} \boldsymbol{Q}_j \boldsymbol{g}_m\right)^{-1}$, $\mu_{0,j}^m = v_{0,j}^m \boldsymbol{g}_m^{\mathrm{t}} \boldsymbol{Q}_j \boldsymbol{e}_{j,m}$, $v_{1,j}^m = \left(\boldsymbol{g}_m^{\mathrm{t}} \boldsymbol{Q}_j \boldsymbol{g}_m\right)^{-1}$, $\mu_{1,j}^m = v_{1,j}^m \left(\boldsymbol{g}_m^{\mathrm{t}} \boldsymbol{Q}_j \boldsymbol{e}_{j,m} - \beta_m\right)$. Following [9], we consider an exponential prior for α_m (here we choose $a = 1$) and a Gamma prior for $\beta_m : \mathcal{G}(\beta_m, b, c)$ (here we choose $b = 2$ and $c = 0.1$). Note that the normalizing constant K can be calculated analytically using Parabolic Cylinder functions[1].
Sampling the binary label q_j^m consists first in generating u_j^m from the uniform pdf $\mathcal{U}([0, 1])$ and second in applying the following rule : $u_j^m \leq \lambda_{1,j}^m \Longrightarrow q_j^m = 1$, otherwise $q_j^m = 0$.
The posterior mixture (4) shows that the conditional distribution $p(a_j^m | q_j^m{=}1, \boldsymbol{\theta}_m, \boldsymbol{y})$ is not standard and so more complex to sample. To solve for this problem, we resort to a Metropolis-Hastings algorithm in which the instrumental pdf is a truncated normal distribution as in [9]. The sampling of this truncated normal pdf is done using an accept-reject sampling algorithm [10].

3.3.3. The noise variances.

Sampling the noise variances $\boldsymbol{\sigma}_{\boldsymbol{\varepsilon}}^2$ can be performed in parallel. Drawing a sample from $p(\sigma_{\varepsilon_j}^2 \mid rest)$ is straightforward since this pdf is an inverse Gamma distribution : $p(\sigma_{\varepsilon_j}^2 \mid rest) \sim \mathcal{IG}((N + 1 - Q)/2, \|\widetilde{\boldsymbol{y}}_j\|^2_{\boldsymbol{I}_N - \boldsymbol{P}\boldsymbol{P}^{\mathrm{t}}}/2)$.

3.3.4. The weighting probabilities.

Sampling the probabilities $\boldsymbol{\lambda} = (\lambda_m)_{m=1:M}$ can also be parallelized. Drawing a realization of λ_m consists in sampling from a beta pdf : $p(\lambda_m \mid \boldsymbol{q}^m) \sim \mathcal{B}(J_{1,m} + 1.5, J_{0,m} + 1.5)$, where $\boldsymbol{q}^m = (q_j^m)_{j=1:J}$. For every condition m, $C_{1,m}$ and $C_{0,m}$ stand for the sets of activated and unactivated voxels, respectively and $J_{i,m} = \mathrm{Card}\,[C_{i,m}]$, with $\sum_i J_{i,m} = J$.

3.3.5. The mixture parameters.

The variance of class 0 follows an inverse Gamma pdf :
$p(v_{0,m} \mid \boldsymbol{z}^m) \sim \mathcal{IG}\big((J_{0,m} - 1)/2, \nu_{0,m}/2\big)$, where :
$\nu_{0,m} = \sum_{j \in C_{0,m}} (a_j^m - \eta_{0,m})^2$ and $\eta_{0,m} = J_{0,m}^{-1} \sum_{j \in C_{0,m}} a_j^m$.
Sampling the hyperparameters (α_m, β_m) is done as in [9] using a Metropolis-Hastings algorithm for α_m with a Gamma instrumental density and simulating β_m according to a Gamma distribution (for more details see [9]).

4. SIMULATION RESULTS

We tested our method on simulated artificial fMRI data and compared it to previous work [3]. We simulated a random inter mixed sequence of indexes coding for $M = 2$ different stimuli. Two sets of trials were thus generated, each of them corresponding to a specific stimulus. These binary time series were multiplied by a stimulus-dependent scale factor. The ROI $\mathcal{R}$ consisted of $J = 60$ voxels, with $J_{1,1} = 34$ activated voxels for condition 1, corresponding to voxels 20 to 53 in Fig 1(b) ($J_{0,1} = 26$) and $J_{1,2} = 22$ activated voxels for condition 2, corresponding to voxels 23 to 38 and voxels 55 to 60 in Fig 1(d) ($J_{0,2} = 38$). We decided to simulate positive NRLs using Gamma distributions : $\boldsymbol{a}^1_{j \in C_{1,m=1}} \sim \mathcal{G}(\alpha_1 = 3, \beta_1 = 1)$ (lower signal to noise ratio for condition 1), $\boldsymbol{a}^2_{j \in C_{1,m=2}} \sim \mathcal{G}(\alpha_2 = 10, \beta_2 = 2)$, and $\boldsymbol{a}^{1,2}_{j \in C_{0,m}} \sim \mathcal{N}(0, \sigma^2_{0,m} = 0.1)$.
For all voxels, the binary stimulus sequence was convolved with the canonical HRF $\boldsymbol{h}_c$[2], whose exact shape appears in Fig. 1(a) in ■-line. A white Gaussian noise $\boldsymbol{b}_j$ was then added to the stimulus-induced signal $\sum_m a_j^m \boldsymbol{X}^m \boldsymbol{h}$ in every voxel V_j. Space-varying low-frequency drifts $\boldsymbol{P}\boldsymbol{\ell}_j$ (generated from a cosine transform basis which coefficients $\boldsymbol{\ell}_j$ are drawn from a normal distribution) were also added to the fMRI time courses.
Fig 1(b)-(c) show the estimated NRLs for the first condition in all voxels using a two-Gaussian mixture model (2GM) and the Gamma-Gaussian model (GGaM), respectively. Fig 1 (d)-(e) illustrate the behavior of these estimates for the second condition. Using the GGaM, we get a more accurate estimation of both the NRLs (smaller errors bars and lower mean square error) and the labels, while no significant difference allows to discriminate the HRF estimates, both being very close to the true HRF shape. Fig 1 (e)-(f) show the posterior mean estimates $\bar{p}_j^m = \frac{1}{K_0 - I + 1} \sum_{k=I}^{K_0} (q_j^m)^k$, of the posterior probability $p(q_j^m = 1 \mid \boldsymbol{y})$ of deciding voxel V_j lies in class 1 for condition m (symbols $*$ and $\circ$ represent these values for both prior mixture models GGaM and 2GM, respectively). This means that when $\bar{p}_j^m < 0.5$, V_j is considered as unactivated. These results confirm what we expected : using GGaM, we observe a higher value of $\bar{p}_j^m$ when V_j is truly activated for condition m and a lower value otherwise.
Finally, Fig 1(f) compares the sensitivity of both models. It is shown that 4 false negative voxels (voxels declared as unactivated while they belong to class 1) are estimated by 2GM, while only one voxel is retrieved by the inhomogeneous prior mixture (GGaM). This is emphasized in Fig 1(f) by $\circ$ and $*$ symbols appearing below the $y = 0.5$ dotted line.

5. EXPERIMENTAL RESULTS

Real fMRI data were recorded during an experiment, which consisted of a single session of $N = 125$ scans lasting $\mathrm{TR} = 2.4$ s each. The main goal of this experiment was to quickly map several brain functions. The chosen ROI $\mathcal{R}_1$ is a Statistical Parametric Mapping (SPM) cluster obtained from thresholded t maps at $p = 0.001$ (corrected for multiple comparisons). This cluster results from the "*audio minus video*" comparison that elicits activation when the audio stimulus gives a stronger response than the video one. As a consequence, the voxels in $\mathcal{R}_1$ should not be involved in visual perception a priori. Fig 2(a)-(e) show only the results for the visual stimulus. In $\mathcal{R}_1$, Fig. 2(b)-(c) show the maps of the NRL estimates using 2GM and GGaM, respectively : no major difference is observed between the NRL estimates provided by the different models. Fig 2(d)-(e) demonstrate that a significant

[1] `http ://mahieddine.ichir.free.fr/`

[2] used in SPM2 : `www.fil.ion.ucl.ac.uk/spm/`

decrease of false positive rate is achieved using the GGaM : almost all voxels appear in black (not activated).

6. CONCLUSION

We proposed an extension of [3] to make the detection estimation approach of brain activity more robust. We demonstrated the improvement brought by this extension both on simulated and real fMRI data and specially in terms of decreased false positive rate. Other extensions would consist in modeling the deactivation process with a third class in the mixture, and accounting for the serial correlation of fMRI data using an AR(1) model as in [4].

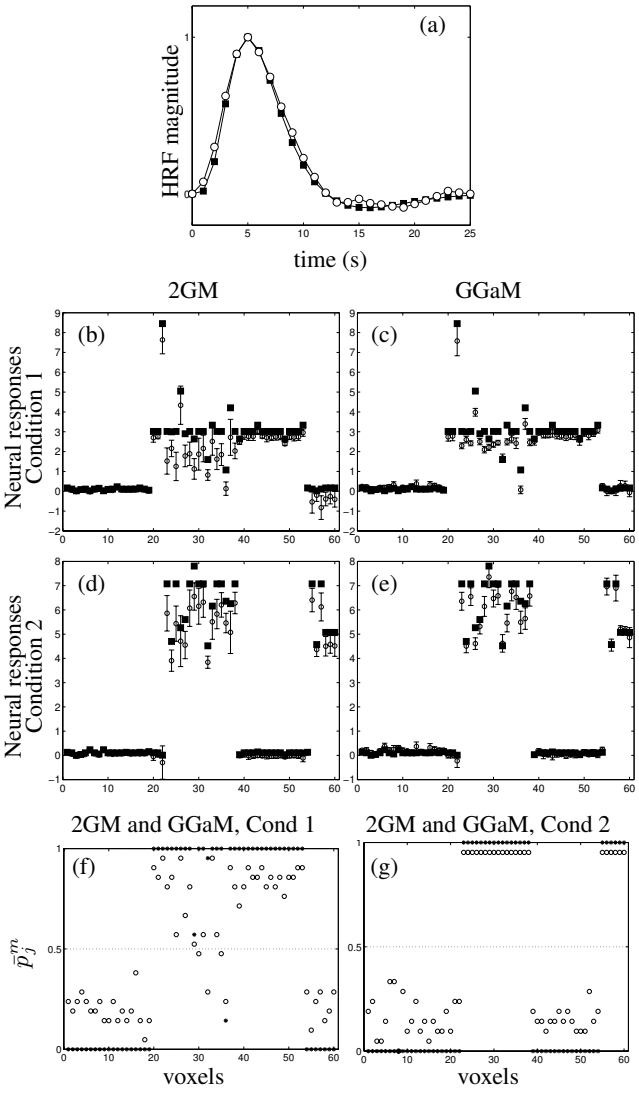

Fig. 1. (a) true HRF $\boldsymbol{h}_c$ (■-), HRF estimate (same result using 2GM and GGaM) (○-).(b)-(c) NRL estimates a_j^1 using the 2GM and the GGaM, respectively. Symbols ■ and ○ correspond to true and the estimated NRL values, respectively. (d)-(e) Same results for a_j^2. (f)-(g) $\bar{p}_j^1$ and $\bar{p}_j^2$, where symbols $*$ and ○ correspond to GGaM and 2GM, respectively. The error bars are derived from the sampled posterior variances of the NRLs.

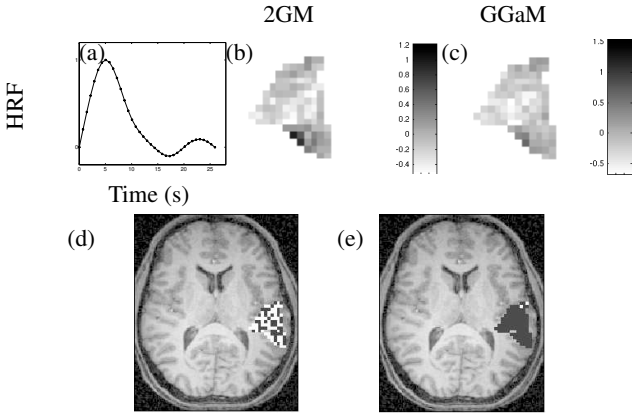

Fig. 2. (a) HRF estimate for $\mathcal{R}_1$ (same result using 2GM and GGaM). (b)-(c) The video NRL estimates using the 2GM and GGaM respectively. (d)-(e) Classification maps for the visual condition in $\mathcal{R}_1$ using the 2GM and GGaM respectively (dark : class 0, white : class 1).

7. REFERENCES

[1] P. Ciuciu, J.-B. Poline, G. Marrelec, J. Idier, C. Pallier, and H. Benali, "Unsupervised robust non-parametric estimation of the hemodynamic response function for any fMRI experiment," *IEEE TMI*, vol. 22, no. 10, pp. 1235–1251, 2003.

[2] M. Woolrich, M. Jenkinson, J. Brady, and S. Smith, "Fully Bayesian spatio-temporal modelling of fMRI data," *IEEE Trans. Med. Imag.*, vol. 23, no. 2, pp. 213–231, February 2004.

[3] S. Makni, P. Ciuciu, J. Idier, and J.-B. Poline, "Joint detection-estimation of brain activity in functional MRI : a multichannel deconvolution solution," *IEEE Trans. Signal Processing*, vol. 53, no. 9, pp. 3488–3502, Sep. 2005.

[4] S. Makni, P. Ciuciu, J. Idier, and J.-B. Poline, "Joint detection-estimation of brain activity in fMRI : an extended model accounting for serial correlation," Tech. Rep., CEA/SHFJ, 2005.

[5] N. Vaever Hartvig and J. Jensen, "Spatial mixture modeling of fMRI data," *HBM*, vol. 11, no. 4, pp. 233–248, 2000.

[6] B. S. Everitt and E. T. Bullmore, "Mixture model mapping of brain activation in functional magnetic resonance images," *Hum. Brain Mapp.*, vol. 7, pp. 1–14, 1999.

[7] R. Buxton and L. Frank, "A model for the coupling between cerebral blood flow and oxygen metabolism during neural stimulation," *J. CBFM*, vol. 17, no. 1, pp. 64–72, 1997.

[8] G. Marrelec, P. Ciuciu, M. Pélégrini-Issac, and H. Benali, "Estimation of the hemodynamic response function in event-related functional MRI : Bayesian networks as a framework for efficient bayesian modeling and inference," *IEEE Trans. Med. Imag.*, vol. 23, no. 8, pp. 959–967, Aug. 2004.

[9] S. Moussaoui, D. Brie, C. Carteret, and A. Mohammad-Djafari, "Application of Bayesian Non-negative Source Separation to Mixture Analysis in Spectroscopy," presented at MaxEnt04, 25-30 July 2004, Germany.

[10] V. Mazet, D. Brie, J. Idier, "Simuler une distribution normale à support positif à partir de plusieurs lois candidates," GRETSI 2005, 6-9 Sep. 2005, Louvain-la-Neuve, Belgique.